Superconductivity for Improved Microwave Ferrite Devices

Gerald F. Dionne, Daniel E. Oates, Donald H. Temme, and Jerald A. Weiss

We have demonstrated a new class of radio frequency (RF) devices that combine low-insertion-loss superconductor circuits with variable magnetization ferrites. The devices are designed to prevent penetration of the superconductor by DC magnetic fields associated with the ferrite, thus preserving the low RF loss of the superconductor while allowing interaction of the RF magnetic fields with the magnetized ferrite. A prototype ferrite-superconductor phase shifter that employs high-T_c $YBa_2Cu_3O_7$ (YBCO) superconductor meanderlines has produced over 700° of differential phase shift at 9 GHz with a figure of merit exceeding 1000°/dB over a 2-GHz-wide frequency band. We have also demonstrated a three-port switching circulator by combining three low-loss superconductor meanderline sections with alternating T junctions on a ferrite substrate. This innovative adaptation of two important technologies promises performance advantages that include lower insertion loss and reduced size and weight, compared to conventional techniques. By optimizing ferrite properties for use at cryogenic temperatures, we also expect to achieve lower switching energies and faster switching speeds.

Since the discovery of high-T_c superconductors in 1986, a major thrust in the development of these materials has been for microwave applications. With increasingly refined thin-film deposition techniques, the radio frequency (RF) surface resistance of superconducting $YBa_2Cu_3O_7$ (YBCO) films at 77 K is now much lower than that of conventional conductors, up to frequencies of at least 100 GHz [1]. This achievement has been exploited to develop a wide variety of miniature passive microwave components, as described in this journal in a companion article by W.G. Lyons et al. In this article we present work on a new class of active planar RF devices that exploit the low insertion loss of superconductor circuits and the unique magnetic properties of ferrite substrates. These devices, which include microwave phase shifters and circulators, have applications in a broad range of military and commercial microwave systems, and offer important size, weight, and performance advantages over conventional microwave technology.

Ferrite components have been widely employed in microwave systems for many years. Adjustable phase shifters, for example, are the principal beam-steering component of agile-beam phased-array radars such as the ground-based Patriot and shipboard Aegis systems. Ferrite circulators are used in radar systems to isolate transmitters from reflected energy and to direct return signals into receiver channels. Circulators can also be employed as switches in selective filter banks. These devices are based on unique microwave phase-shift properties that are the result of gyromagnetic effects. The phase shift of an RF wave traversing the ferrite can be controlled by applying a small magnetic field to adjust the ferrite magnetization.

Superconductive RF circuits overcome the limitations of present-day planar circuit components by virtually eliminating conduction losses. To avoid excessive conduction losses, devices based on normal metal conductors such as copper or gold must be configured in waveguides rather than the more compact microstrip or planar stripline geometries. In our work with superconductor microstrip circuitry, we have demonstrated that miniature low-loss ferrite devices can be realized, and these devices offer an attractive replacement for bulky waveguide systems. As we show, these devices provide dramatically improved figures of merit, or degrees of phase shift per dB of loss, compared to conventional microwave devices. Furthermore, the reduced device size results in lower switching energies and shorter switching times. Devices based on high-T_c superconducting films operate at temperatures between 50 and 90 K, and thus can utilize small, reliable, power-efficient closed-cycle cryocoolers that have been developed for operation in this temperature range.

An advantage of operating ferrite devices at cryogenic temperatures is the improvement in key properties of the ferrite material. At low temperatures, for example, ferrite saturation magnetization limits can be increased substantially, extending the range of efficient phase-shift operation to RF frequencies higher than those available at room temperature.

One of the technical challenges in realizing superconductor ferrite devices is the development of component designs that avoid magnetic-field penetration of the superconductor. Applied magnetic fields are central to device operation because these fields control the ferrite RF properties. However, magnetic-field penetration of a superconductor can lead to deterioration of the superconducting properties [2]. For device designs in which significant magnetic fields penetrate the circuit, superconductivity would have no advantage over the normal conductivity of copper at 77 K [3]. This article describes our development of ferrite-superconductor devices that eliminate magnetic-field penetration, thus preserving the favorable superconducting properties. The results of our experiments confirm that ferrite-superconductor devices can be realized and they can operate with negligible conduction losses in the microwave frequency bands.

Gyromagnetic Effects

Gyromagnetism is the basic phenomenon that enables magnetic control of the phase of RF waves in gyrotropic media such as ferrites. In applying Maxwell's equations to analyze the propagation of a plane wave in a magnetized ferrite medium, we must first recognize that an RF component of magnetization is induced by the RF magnetic-field component and that the associated RF permeability contains dispersive and dissipative terms. These terms arise from a tensor that results from gyromagnetic effects (ferrimagnetic resonance), but the permeability can be approximated as a complex scalar quantity for the purposes of our device analyses [4]. Therefore, we define the RF permeability as

$$\mu = \mu' - j\mu''.$$

When μ is introduced into the expression for the complex RF propagation constant $\Gamma = \alpha + j\beta$ in the frequency regimes of interest, the absorption constant α depends primarily on μ'', and for $\mu' \approx 1$ is given by

$$\alpha \approx \frac{1}{2}\frac{2\pi\sqrt{\varepsilon}}{\lambda}\mu'',$$

where ε is the dielectric constant of the ferrite and λ is the free-space RF wavelength. The phase constant β depends primarily on μ', and for $\mu'' \approx 0$ is given by

$$\beta \approx \frac{2\pi\sqrt{\varepsilon}}{\lambda}\sqrt{\mu'}. \quad (1)$$

The corresponding phase change ϕ of a wave traversing a distance L through the ferrite equals βL. With the approximation in Equation 1 we can express ϕ as

$$\phi \approx 2\pi\sqrt{\varepsilon\mu'}\,\frac{L}{\lambda}. \quad (2)$$

The RF absorption by the ferrite is usually characterized by the magnetic loss tangent

$$\tan\delta_\mu = \frac{\mu''}{\mu'}. \quad (3)$$

The relations for the frequency dependence of μ' and μ'' originate from the classical analysis of a magnetization vector precessing at an angular frequency $\omega_0 = 2\pi\nu_0$ about a DC magnetic-field vector of magnitude H. The sense of the precession is determined by the direction of the magnetic-field vector, and the frequency ν_0 is proportional to H. When the frequency ν of the RF magnetic field matches the precession frequency (i.e., when $\nu = \nu_0$), ferrimagnetic resonance occurs. This effect can be visualized if a linearly polarized wave with the RF magnetic-field component normal to the magnetization vector is analyzed in terms of two counterrotating circularly polarized components, one rotating in synchronism with the precession (labeled +) and the other in opposition to it (labeled –). The propagation of the two polarizations differs as a function of frequency, with the + component undergoing the resonance effect. Distinct permeabilities μ_+ and μ_- can then be defined for use in Equations 1, 2, and 3. For devices that utilize circularly polarized waves, the difference between the two permeabilities can be exploited to produce significant phase-shift effects, as we show later.

As derived from a mathematical analysis of the permeability tensor, the real and imaginary permeability components for the two circular polarizations are expressed as

$$\mu'_\pm = 1 + \frac{\gamma(4\pi M)(\nu_0 \mp \nu)}{(\nu_0 \mp \nu)^2 + (\Delta\nu_0)^2} \tag{4}$$

and

$$\mu''_\pm = \frac{\gamma(4\pi M)\Delta\nu_0}{(\nu_0 \mp \nu)^2 + (\Delta\nu_0)^2}, \tag{5}$$

where $\nu_0 = \gamma H$ is the ferrimagnetic resonance frequency, $\Delta\nu_0$ is the intrinsic half-linewidth resulting from magnetic resonance damping, $\gamma = 2.8$ GHz/kG is the gyromagnetic constant, and M is the magnitude of the DC magnetization vector [4]. Recalling that the + and – polarizations are determined by the sense of the precessing magnetization vector, we note that a reversal in the direction of the vector will cause μ_+ and μ_- to be interchanged. From Equations 4 and 5, at a given frequency there are two ways to alter the permeability: (1) by varying ν_0 through control of the external magnetic field H, or (2) by changing $\gamma(4\pi M)$ through adjustment of the magnetization M, which can be varied over a range from zero (complete demagnetization) to $4\pi M_s$ (full magnetic saturation).

In our work on ferrite devices, we emphasize RF waves having circular polarization, since this polarization can provide much larger phase shifts than linear polarization. Figure 1 shows an example of the variation with respect to ν_0 of the ferrite complex permeability for circularly polarized waves of fixed frequency ν equal to 10 GHz. To avoid high absorption near the resonance peak in μ''_+, the resonance frequency ν_0 is set far from ν. To maximize the useful frequency band of operation, the ferrite is chosen with $\Delta\nu_0$ small enough to be ignored in the denominator of Equations 4 and 5. When the resonance frequency ν_0 is small with respect to ν, there is a significant difference between the permeabilities μ'_+ and μ'_- for the two senses of circular polarization. Under these conditions, Equation 4 can be reduced to

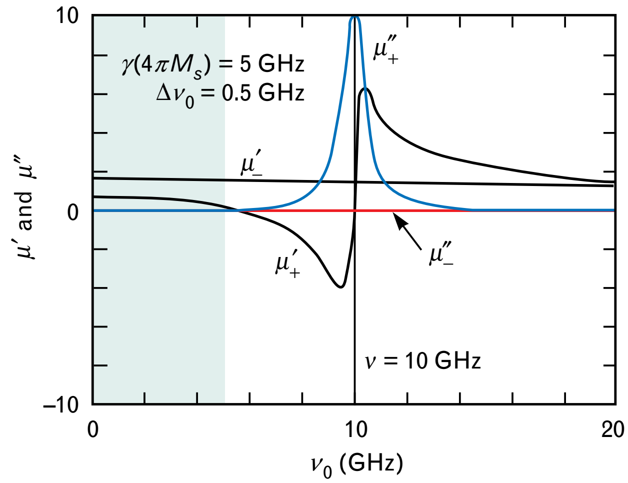

FIGURE 1. Variation of the four complex permeability components for circular polarization as a function of the ferrimagnetic resonance frequency ν_0 for a fully magnetized ferrite with $\gamma(4\pi M_s)$ = 5 GHz and the half-linewidth $\Delta\nu_0$ = 0.5 GHz (broadened for illustration purposes). The RF frequency ν for this example is 10 GHz. The magnitude of the difference between μ'_+ and μ'_-, which is related to the magnitude of the differential phase shift, is greater and less frequency sensitive in the regime where $\nu_0 << \nu$, compared to the regime where $\nu_0 >> \nu$. In this example, the shaded region indicates the range of resonance frequencies acceptable for device operation.

$$\mu'_\pm \approx 1 \mp \frac{\gamma(4\pi M)}{\nu}. \tag{6}$$

Devices that operate in this regime with circularly polarized waves are therefore described as nonreciprocal, because forward and reverse directions of propagation have different permeabilities and propagation constants. The corresponding difference in phase,

$$\Delta\phi = \phi_+ - \phi_- = 2\pi\sqrt{\varepsilon}\left(\sqrt{\mu'_+} - \sqrt{\mu'_-}\right)\frac{L}{\lambda},$$

obtained by reversing the direction of the signal propagation or, more conveniently, reversing the direction of the magnetization vector is called the *differential phase shift*.

For the case in which both ν_0 and $\gamma(4\pi M)$ are much less than ν, we can use Equations 3 and 6 to express the differential phase shift and the magnetic loss tangent as

$$\left|\Delta\phi\right| \approx 2\pi\sqrt{\varepsilon}\,\frac{\gamma(4\pi M)}{\nu}\,\frac{L}{\lambda}$$

and

$$\tan\delta_\mu \approx \frac{\gamma(4\pi M)}{\nu}\,\frac{\Delta\nu_0}{\nu}.$$

From these relations, we see that the design objective is to employ the ferrite with the largest $4\pi M_s$, for maximum phase shift, and the narrowest $\Delta\nu_0$, for minimum loss tangent. There is a limitation on the values of $4\pi M_s$, however, arising from the magnetic fields that occur among the domains in partially magnetized ferrite. These internal fields range in magnitude from zero to $4\pi M_s$ and create absorption losses over the frequency band from zero to $\gamma(4\pi M_s)$. Since this low-field-loss regime must be avoided for devices,

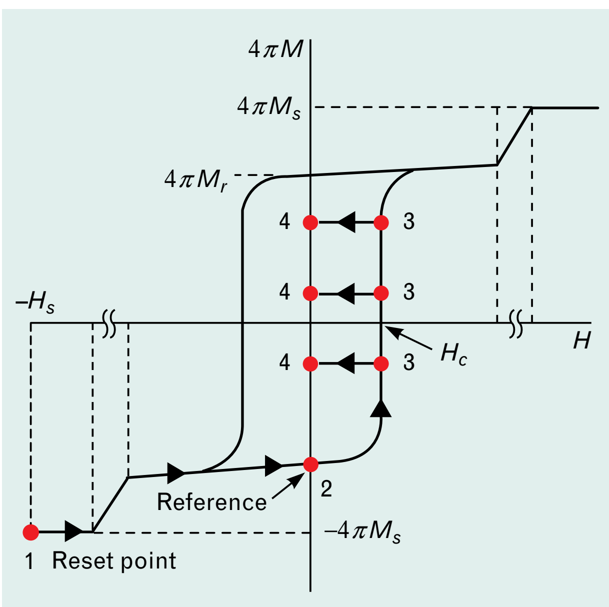

FIGURE 2. Hysteresis-loop principle for magnetic-flux switching (flux-drive method) of microwave ferrite phase shifters. The important features of this loop are the remanence ratio $4\pi M_r/4\pi M_s$, which should be as large as possible, and the coercive field H_c, which should be as small as possible.

the ferrite selected for a particular application requires a value of $4\pi M_s$ low enough to allow efficient operation in the desired frequency band.

For most applications, the relation

$$\frac{\gamma(4\pi M_s)}{\nu} \le 0.5 \qquad (7)$$

defines the practical limit to avoid low-field-loss effects, and is generally used as a device design goal for maximum efficiency. Ferrites with saturation magnetization $4\pi M_s$ ranging up to 5 kG at room temperature can be obtained commercially for the lower microwave frequency bands. Since this limit on $4\pi M_s$ corresponds to a gyromagnetic frequency of 14 GHz, the maximum operating frequency for which the above ratio can be achieved is 28 GHz. For frequency increases beyond 28 GHz, concerns about low-field loss disappear because the relation in Equation 7 is always satisfied. However, the frequency limit for optimum phase-shift efficiency can be raised substantially higher than 28 GHz by cooling the ferrite to cryogenic temperatures where values of $4\pi M_s$ exceeding 7 kG are attainable.

Magnetization Control

For typical phase shifters and junction circulators that operate in the partially magnetized state, the value of $\Delta\phi$ is directly related to $4\pi M$, which in turn is established by the device operating point on the ferrite hysteresis loop. Figure 2 illustrates the key features of the ferrite hysteresis loop, which shows the dependence of magnetization on the magnetic field. The remanent magnetization $4\pi M_r$, which has a value in the magnitude range $0 < 4\pi M_r < 4\pi M_s$, is defined as the level of magnetization that remains after a magnetizing field is removed. The remanence ratio, which is the ratio of $4\pi M_r$ to the saturation magnetization $4\pi M_s$, is typically 0.7 for ceramics with randomly oriented crystal grains. The coercive field H_c should be as small as possible to ensure low switching energies and switching times. In systems applications that employ remanent-state variable phase shifters, such as phased-array radars, the parameters of the hysteresis loop are critically important.

The desired magnetization level can be established through the use of fixed-voltage impulses of controlled duration applied through a magnetizing coil to generate variable amounts of magnetic-flux reversal (the flux-drive method) [5]. The ferrite is set to remanence at $-4\pi M_r$ on its major hysteresis loop by first applying a saturating impulse of field $-H_s$ (reset point 1 in Figure 2) and then allowing the magnetization to relax to its maximum remanence value (reference point 2, the latching condition). Selected voltage impulses of shorter length bring the magnetization to points 3 on a minor loop by reversing predetermined amounts of flux. The magnetization then attains the corresponding new remanent states (points 4) after each pulse is completed. We can follow this procedure to obtain any value of $4\pi M$ within the range available to the device. By resetting to point 1 and reestablishing point 2 before each new pulse is applied, we can exploit the full range of magnetization ($-4\pi M_s$ to $+4\pi M_s$) without the use of holding currents.

Ferrite-Superconductor Devices

To join a ferrite to a superconductor without allowing magnetic fields associated with the magnetization of the ferrite to penetrate the superconductor and degrade its properties, we used a design based on magnetic-flux confinement within a closed magnetic circuit, e.g., ferrite in a toroidal geometry, as illustrated in Figure 3. In effect there are no magnetic poles on the ferrite surface to produce an external magnetic field, and the superconductor can be in contact with any surface of the magnetized toroid. The only other basic requirement for gyromagnetic interaction is for the RF magnetic field to be normal to the magnetization vector of the ferrite. This relationship between magnetization and field is usually achieved in microstrip circuits by maintaining the magnetization along the direction of signal propagation. The magnetization level, and hence the amount of phase shift, is controlled by applying electrical impulses to the magnetizing coil, as described in the previous section.

Phase Shifters

We investigated several different configurations of ferrite-superconductor phase shifters to demonstrate their performance advantages. These configurations all comprised compact low-loss superconducting transmission lines in contact with a ferrite magnetized in a closed flux loop, and included a means to adjust the magnetization level for controlling the amount of phase shift. In this section we describe three of these device structures.

Figure 3 illustrates the simplest device design. A one-inch-long niobium superconducting transmission line, deposited on an Al_2O_3 dielectric substrate, is pressed in direct contact with a ferrite (yttrium iron garnet, $Y_3Fe_5O_{12}$, or YIG) rectangular-shaped toroid. A ground plane is deposited on the top surface of the

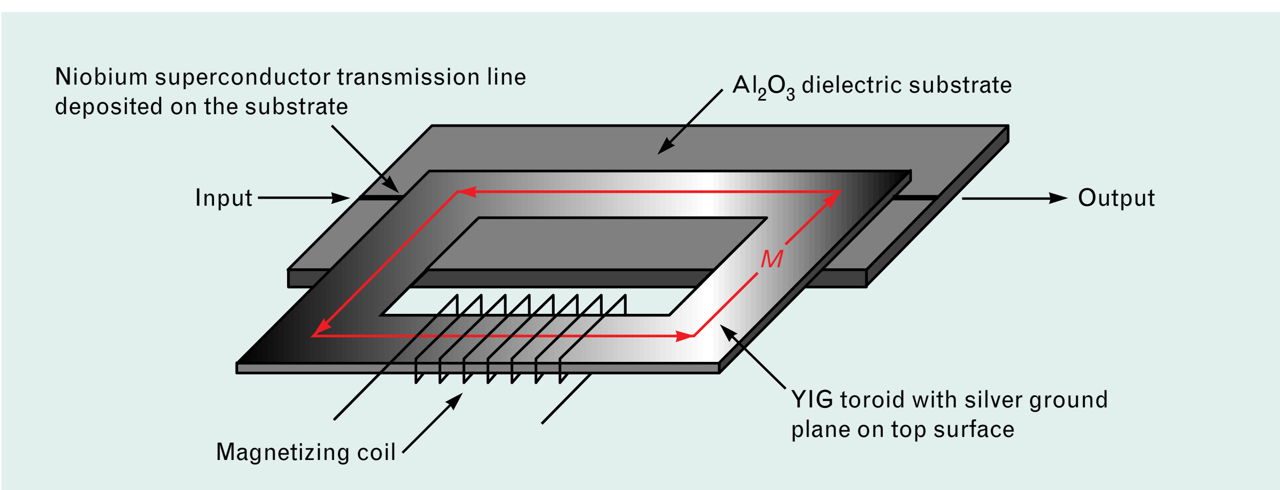

FIGURE 3. Structure of an experimental reciprocal phase shifter showing the coupling relationship between magnetized ferrite (yttrium iron garnet, $Y_3Fe_5O_{12}$, or YIG) in the shape of a planar rectangular-shaped toroid and the niobium superconductor transmission line on an Al_2O_3 dielectric substrate. Magnetic flux is confined within the YIG toroid.

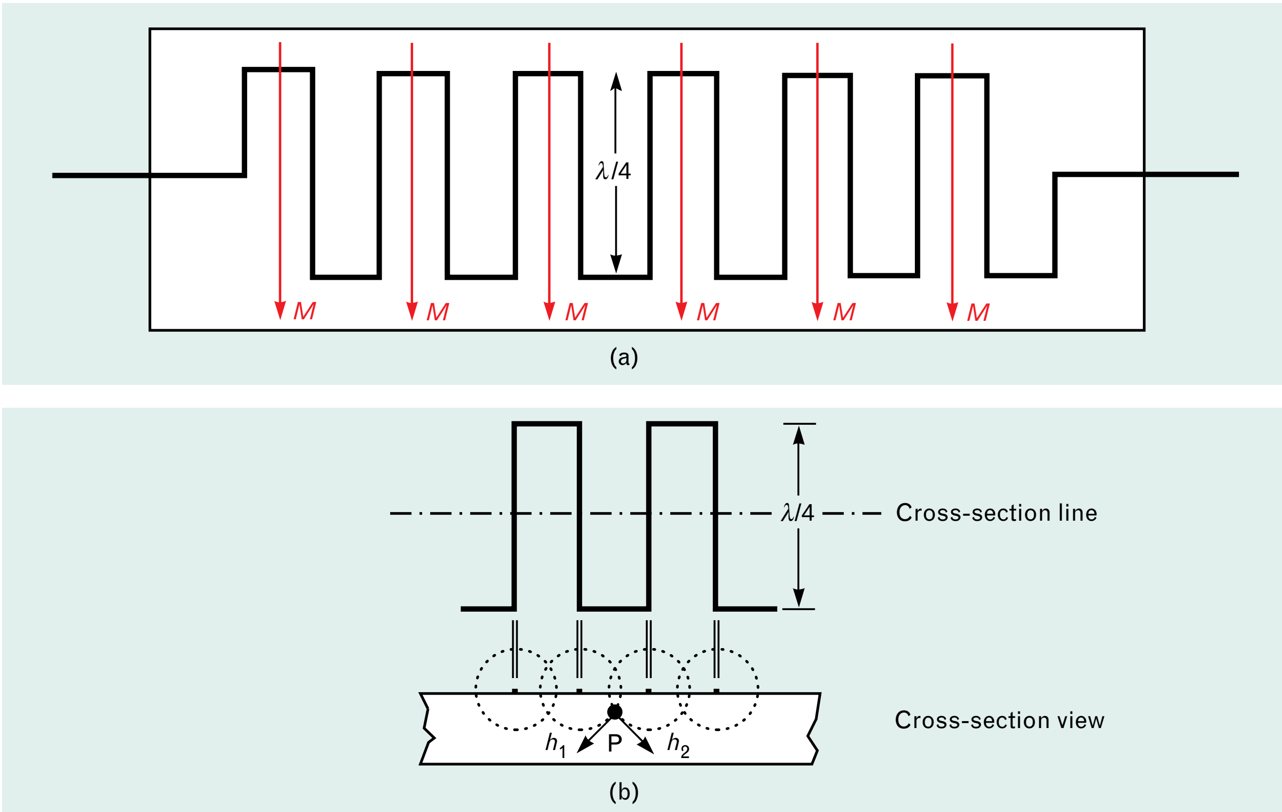

FIGURE 4. Meanderline structure showing the internal generation of circular polarization. (a) Plan view of a meanderline circuit on a ferrite substrate, with magnetization vectors of magnitude M parallel to the meanders. (b) Cross-section view through the meanderline circuit in part *a*, showing the generation of circular polarization at a point P centered between adjacent meanders. The quantities h_1 and h_2 are adjacent-leg RF components of the magnetic field 90° apart in phase along the centerline of the meanderline circuit.

toroid. Since a portion of the RF signal in the superconducting transmission line traverses the ferrite, the gyromagnetic interaction between the magnetic-field component of the RF wave and the magnetized ferrite results in a phase shift that varies with the ferrite magnetization level. In this case, because the RF wave is linearly polarized, the phase shift is reciprocal. Experiments to validate the superconducting RF properties of this initial design of the phase shifter were carried out at 4 K [6]. Measurements indicated that no increase in transmission-line RF loss occurred because of the presence of the magnetized toroid.

As we discussed earlier, much larger phase shifts can be achieved in ferrites by exploiting the nonreciprocal propagation of circular polarization. In planar configurations, we can produce regions of circularly polarized RF field by using a meanderline structure of the type illustrated in Figure 4. When the meander length is near a quarter wavelength, as indicated in the figure, there is approximately a 90° phase difference between signals on adjacent legs of the meander near the centerline of the structure. Overlap of the fields results in circular polarization over a portion of the ferrite cross section between them. The magnetization vector of magnitude M is directed parallel to the meanders to provide a gyromagnetic effect. While meanderline structures have been previously demonstrated for ferrite phase shifters [7–9], the high transmission losses that occur with normal metal conductors have prevented their widespread application.

To demonstrate further the enabling capabilities of superconductivity, we designed a ferrite phase shifter that incorporates a superconducting meanderline circuit to produce circular polarization effects with minimal conduction losses [10–12]. The design was

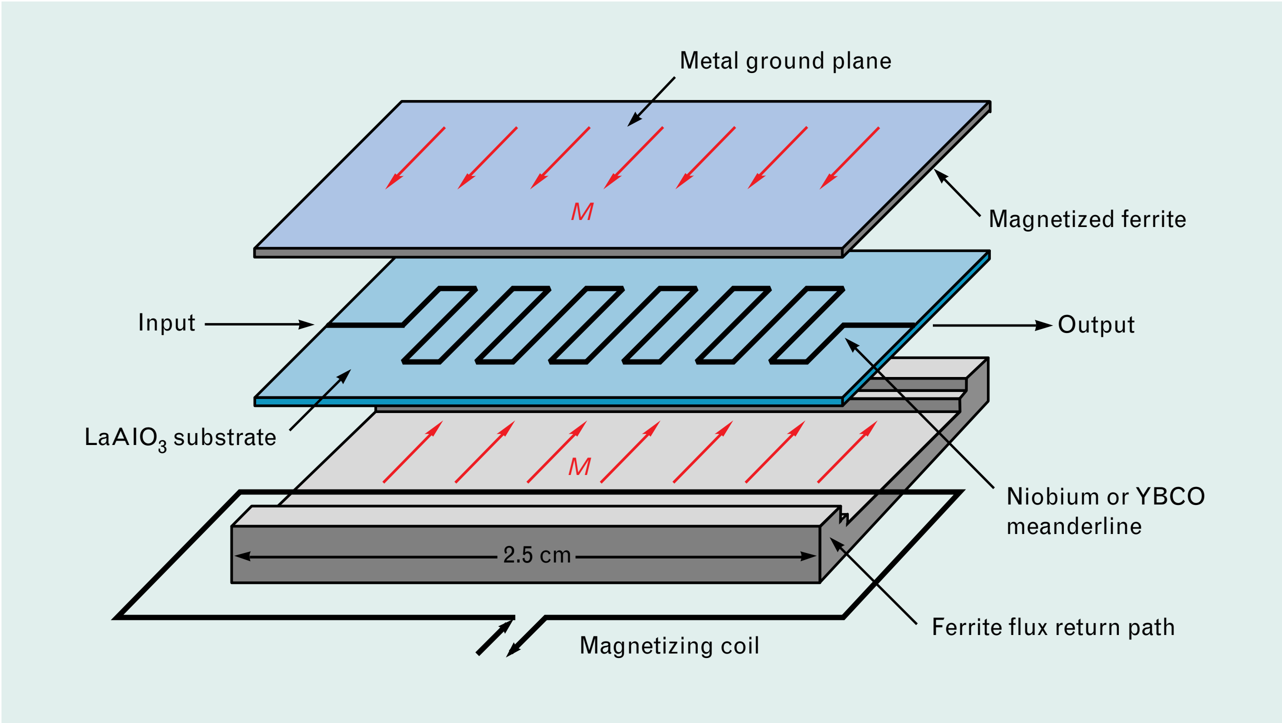

FIGURE 5. Experimental layered phase shifter with meanderline superconductor (niobium or YBCO) deposited directly on a $LaAlO_3$ substrate rather than directly on the ferrite substrate. The ferrite is held in close proximity to the superconductor meanderline. This configuration is necessary in the case of the YBCO circuit.

implemented, as shown in Figure 5, with a high-T_c YBCO superconductor transmission line deposited on a lanthanum aluminate ($LaAlO_3$) substrate, for operation at 77 K. The magnetic circuit, consisting of two parts joined together, forms a toroid of rectangular cross section that establishes the necessary magnetization direction parallel to the meanders. Magnetization control is provided by applying voltage impulses to the magnetizing coil. The meanderline is held in contact with the ferrite by "spring fingers," as shown in Figure 6. Ultimately, as materials technology advances, YBCO deposited directly on ferrite will simplify the device design by eliminating the $LaAlO_3$ substrate and therefore the need to hold the YBCO circuit in close contact with the ferrite by mechanical means [13]. At present, YBCO films deposited on $LaAlO_3$ substrates provide superior performance.

We measured both the differential phase shift and insertion loss of the YBCO meanderline phase shifter, confirming the superior figure of merit of ferrite-superconductor devices. The differential phase shift $\Delta\phi$, shown in Figure 7, was determined by measuring the difference in phase between forward-traveling waves and backward-traveling waves for a fixed magnetization direction. The phase shift ranged from 600° to 700° over the frequency band of 8 to 10 GHz. The insertion loss, shown in Figure 8, was less than 1 dB over the 8-to-10-GHz band. After subtracting reflection losses from the data, the absorption losses were less than 0.5 dB over this frequency band. The high absorption region at lower frequencies is caused by ferrimagnetic resonance that occurs when the ferrite is partially magnetized [14, 15]. As discussed earlier, the upper frequency limit of this low-field-loss regime is determined by $\gamma(4\pi M_s)$, which in this case is approximately 5 GHz for the ferrite with $4\pi M_s$ = 1.8 kG at 77 K. The combination of measured phase shift and insertion loss yielded a figure of merit exceeding 1000°/dB over the 2-GHz-wide frequency band.

The phase-shifter results shown in Figure 7 were measured with the ferrite in the remanent state. Measurements to compare the differential phase shift versus frequency between the remanent state and the

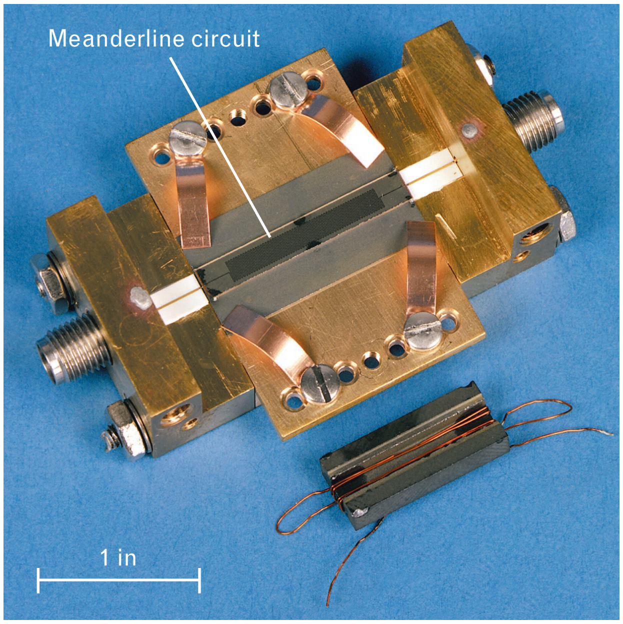

FIGURE 6. YBCO meanderline phase shifter on a $LaAlO_3$ substrate. The ferrite yoke at the bottom has been removed to reveal the meanderline structure.

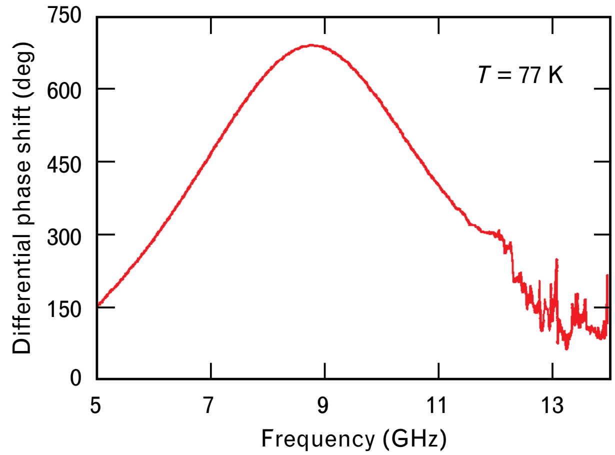

FIGURE 7. Differential phase shift versus frequency for a YBCO meanderline ferrite-superconductor phase shifter on a $LaAlO_3$ substrate, as illustrated in Figure 5.

saturated state were performed on a phase shifter comprising a niobium meanderline deposited on $LaAlO_3$. The results in Figure 9 show that the phase shift versus frequency in the saturated state is about a factor of two greater than the phase shift versus frequency in the remanent state. We can infer from these data that the ferrite remanence ratio is reduced to less than 0.5, which is probably the result of the demagnetizing effects of air gaps in the toroid. Given that the remanence ratio of ferrite is typically 0.7, improved design of the toroid structure should lead to larger phase shifts at the remanent point.

The figure-of-merit values obtained in these experiments can be compared with the 130°/dB remanence value at X-band for a copper meanderline circuit at room temperature [16]. This value is almost an order of magnitude inferior to that of the superconductor devices we have demonstrated. Even at cryogenic temperatures, where the insertion loss from the copper meanderline circuit would decrease by no more than a factor of two, a phase shifter employing superconductors would have at least a factor-of-five advantage in figure of merit. If the theoretical limits of the ferrite properties can be realized in practice, an optimized design with ideal impedance matching of the superconductor circuit and full utilization of $4\pi M_s$, a figure-of-merit value as high as 10,000°/dB is a realistic goal.

To miniaturize device dimensions and optimize the integrity of the magnetic circuit, we have fabricated and tested a planar microstrip phase shifter with a YBCO meanderline circuit deposited on a $LaAlO_3$ substrate, based on the design illustrated in Figure 10. In contrast to a conventional 10-GHz waveguide phase shifter, which is typically about two inches in length, this microstrip device is only a half-inch in length, with a corresponding reduction in cross-sectional area and overall volume and weight. The planar structure still confines the magnetic flux entirely within the ferrite but eliminates the added external yoke. The return path of the flux is outside the meanderline so that the device functions magnetically in a manner identical to the design shown in Figure 5. Because of the simplified structure, this planar device is readily compatible with compact structures in which the superconductor would be in contact with the ferrite through multilayer deposition processes. Figure 11 shows the loss and differential phase shift for the in-plane magnetic circuit. These initial results indicate performance comparable to that achieved for the two-part ferrite structures.

Circulators and Switches

The principles of magnetic and cryogenic design described for the ferrite-superconductor phase shifter

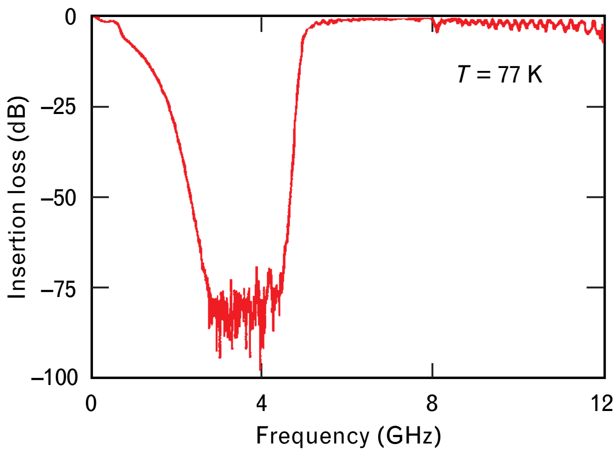

FIGURE 8. Insertion loss versus frequency for the YBCO meanderline ferrite-superconductor phase shifter illustrated in Figure 5. Loss due to reflection effects from impedance mismatches at higher frequencies has not been subtracted.

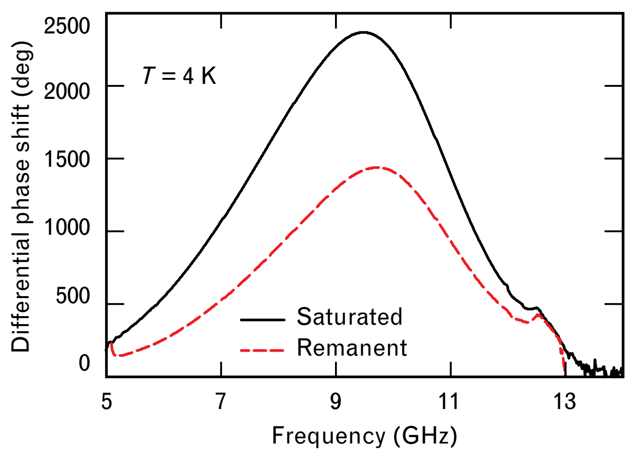

FIGURE 9. Comparison of differential phase shift versus frequency for a niobium meanderline circuit on a $LaAlO_3$ substrate for saturated and remanent states. The device configuration shown in Figure 5 was used to determine these data.

can also be applied to a three-port junction circulator. A style of circulator design that is well adapted to planar circuits, and especially to ferrite-superconductor technology, is the ring-network circulator. The concept was introduced in 1965 [17] and was the subject of experimental investigation at that time [18]. The specific embodiment was a ring composed of three identical nonreciprocal phase shifters alternating with three identical reciprocal T junctions, constituting a three-port junction circulator, as illustrated in Figure 12. This design principle is particularly applicable to miniature planar circuit design, including the ferrite-superconductor combination of superconducting circuit path and planar magnetic-flux confinement, but the formulation is general and valid for any type of microwave or millimeter-wave transmission medium.

The analysis of the ring-network circulator [19, 20] is based on a rigorous scattering formulation of clockwise- and counterclockwise-propagating partial waves. This analysis leads to characterization of the

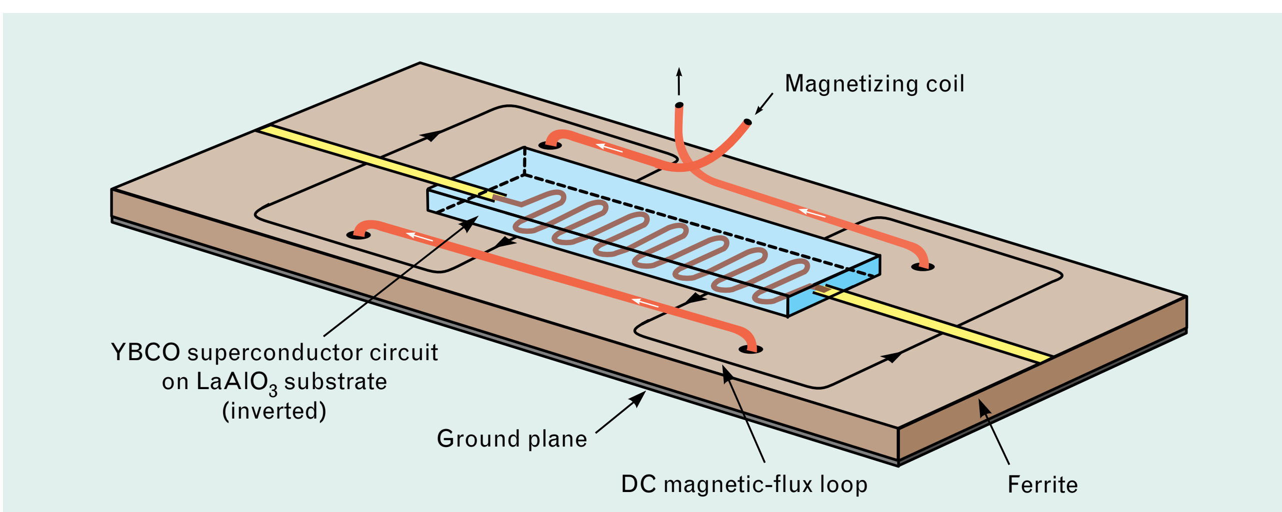

FIGURE 10. A planar microstrip YBCO meanderline phase shifter designed to minimize size and weight and eliminate air gaps in the magnetic-flux path. Such a device would be only a half-inch in length. Tests on devices of this design show results comparable to the larger two-part ferrite structures.

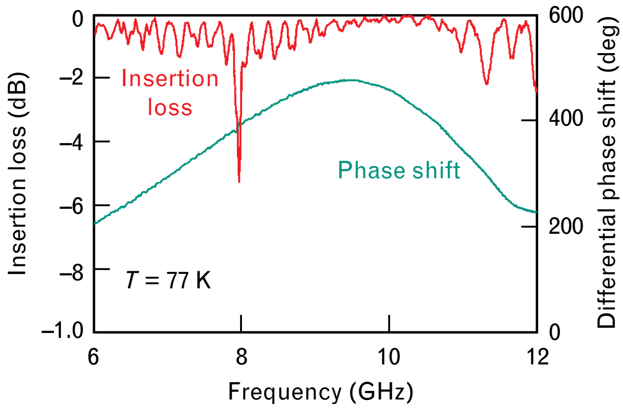

FIGURE 11. Example of insertion loss and differential phase shift versus frequency from a YBCO meanderline circuit on $LaAlO_3$ substrate in a microstrip phase shifter such as the design shown in Figure 10. Excessive ripples in the loss curve are the effects of impedance mismatches in the test circuit.

nonreciprocal phase shift in relation to the T-junction scattering parameters such that, when the phase shifters and T junctions are assembled into a ring, the network satisfies the imposed condition of perfect circulation. Circulator performance over the frequency range in that vicinity is governed by the dispersive characteristics of the components. Computational results indicate that, by suitable design, the required magnitude of differential phase shift can be made small, so as to minimize the amount of gyromagnetic interaction needed. Furthermore, with appropriate choice of dispersive characteristics as specified by the theory (for example, by incorporating reactive elements at the T junctions), the circulator can achieve broadband performance.

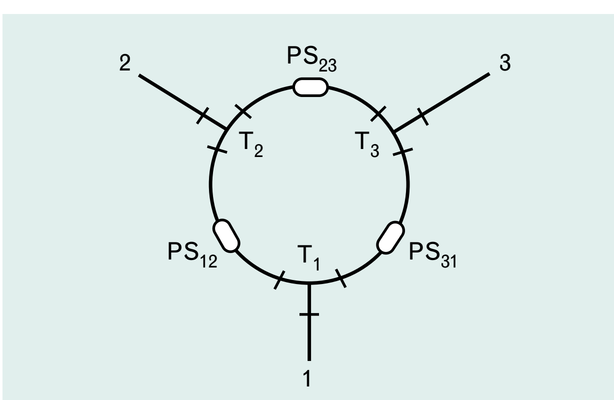

FIGURE 12. Diagram of a ring network. The labels T and PS denote the symmetrical T junctions and the nonreciprocal phase shifters.

Figure 13 shows photographs of an experimental meanderline ring-network circulator. A central hole in the substrate creates the toroidal geometry for flux confinement and accommodates coil windings for establishing and reversing the state of magnetization. The circulator design in Figure 13 is narrowband. Figure 14 shows 10-GHz-band performance data for this device but with a niobium circuit cooled to 4 K. The insertion loss is below 1 dB and isolation is greater than 15 dB over a 2% band. Because the conduction loss due to the niobium superconductor is expected to be less than 0.1 dB for this circuit, we believe that the measured insertion loss is dominated by spurious impedance mismatch effects.

This class of circulator designs confers numerous potential benefits. In contrast to the conventional resonant-type junction circulator in which an external magnetic yoke must be used to magnetize the ferrite element in the direction normal to the plane of the circuit—resulting in degraded performance of the superconductor [3]—the ring-network circulator lends itself naturally to magnetization in the plane of the substrate. The advantages of such a configuration include reduced size, weight, complexity, and energy consumption of the magnetizing structure. Furthermore, the configuration allows for reduced coercivity requirements in self-magnetized versions (i.e., having no external magnet structure) as well as for high-speed energy-efficient switching capability in reversible versions of the circulator, which can function effectively as switches. The minimization of circulator insertion loss through the use of a microstrip superconducting circuit is a major advantage of this design concept.

Materials

The choice of ferrite for a particular application at cryogenic temperatures is determined by the same considerations that apply at room temperature. The saturation magnetization is selected so that $\gamma(4\pi M_s)$ is sufficiently lower than the operating frequency ν such that low-field loss is avoided, as discussed in a previous section. Because $4\pi M_s$ values can increase by more than a factor of two when the material is

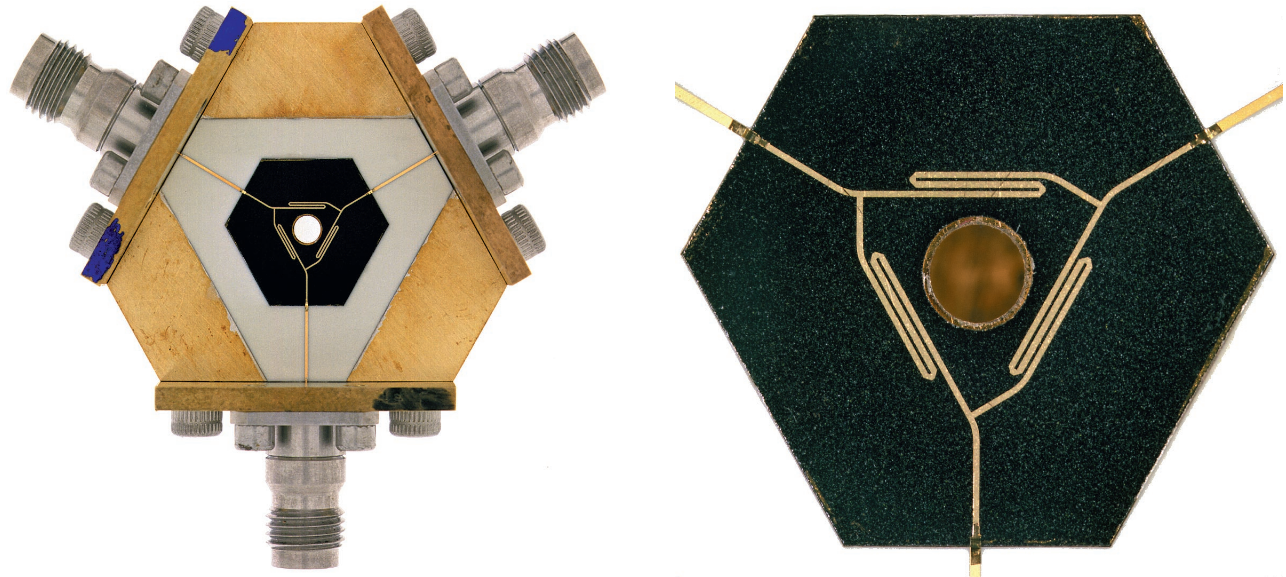

FIGURE 13. Photographs of a ring-network circulator: on the left is a laboratory prototype microstrip circulator with ferrite substrate and meanderline nonreciprocal phase shifters; on the right is an enlarged view of the ring network. The device shown here was fabricated with gold circuitry; the versions of the devices used in the experiments employed niobium superconductor circuits.

cooled from 300 K to 77 K, care must be taken that lower room-temperature magnetization materials be used for the standard microwave frequencies (10 GHz and below). This $4\pi M_s$ enhancement, however, can be an immediate benefit for millimeter-wave designs in which the attainment of $4\pi M_s$ values greater than 5 kG have been a longtime goal.

For cold environments, some commercially available ferrimagnetic spinels and garnets can be used for applications in which the magnetic state is fixed. Where rapid and frequent changes of the magnetic state are expected, however, available materials may not be adequate for achieving high-speed, low switching-energy performance. As shown by the hysteresis loops of yttrium-iron garnet (YIG) in Figure 15, the decrease in temperature from 300 to 77 K causes almost a tenfold increase in the coercive field, due to a rise in the magnetocrystalline anisotropy. At low temperatures, increased stress effects in ferrites can also be a cause of deterioration of the hysteresis loops. If rare-earth impurities are present in any of the chemical constituents, the values of Δv_0 can increase substantially at 77 K and raise the values of $\tan \delta_\mu$ to unacceptable levels. For these reasons, alteration of the chemical compositions of standard room-temperature microwave ferrites will be necessary to attain the highest efficiency. Strategies for accomplishing these materials design changes have been previously established and are well within the capabilities of modern materials technology [21].

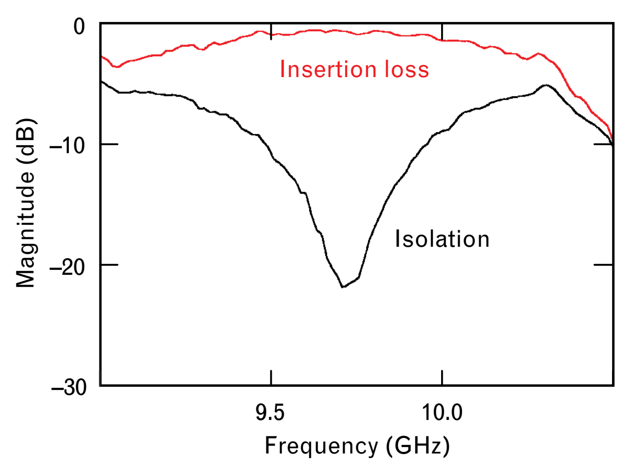

FIGURE 14. Insertion loss and isolation versus frequency measured at the cryogenic operating temperature of 4 K for a ring-network circulator with a niobium superconducting circuit on a ferrite substrate, magnetized circumferentially in its plane. This laboratory prototype is narrowband (about 2% bandwidth at 15-dB isolation) but has favorably low insertion loss (less than 1 dB over that band) and illustrates the feasibility of the ring network as a circulator design concept.

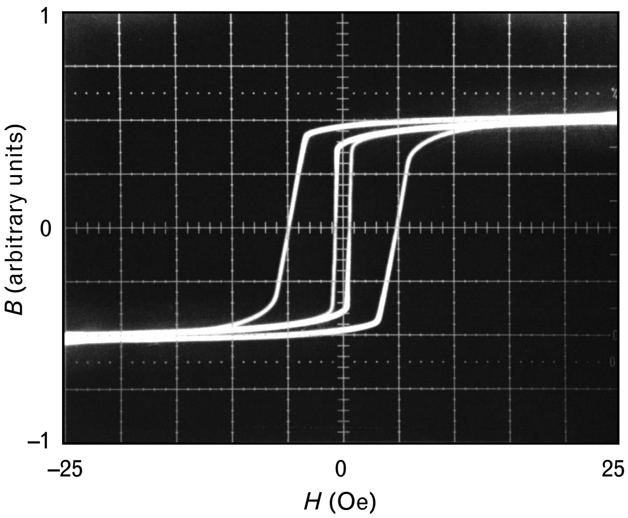

FIGURE 15. Enlargement of a YIG hysteresis loop when T is decreased from 300 to 77 K. The coercive field increases by almost a factor of ten, and the magnetization is enhanced 20% at the remanent point. The 77-K loop is not fully saturated at H = 25 Oe.

For latching operations in which square hysteresis loops are critically important, designs that employ a single-piece ferrite toroid, such as that described previously, might be required to avoid deterioration of the hysteresis-loop squareness caused by gaps that occur where the two ferrite pieces are mechanically joined to form a closed path.

Another objective is to control the physical contact between ferrite and superconductor in order to optimize the interaction between the two and to establish the highest possible reproducibility. Figure 16 illustrates four proposed schemes for achieving the desired configurations. With the use of suitable dielectric buffer layers, the YBCO (or equivalent) superconductor circuit can be established in a controlled proximity to the surface of the ferrite, which can in turn be magnetized with internal flux confinement.

Summary

We have successfully demonstrated the feasibility of employing superconductors in microwave ferrite devices without deterioration of the superconductor properties. This new technology not only offers dramatically improved efficiency, but also makes possible the use of compact lower-cost microstrip structures to replace bulky ferrite waveguide phase shifters.

For systems such as phased-array radars, the order-of-magnitude advantages gained from the superior performance and reduced size and weight of the ferrite-superconductor technology can make it the pre-

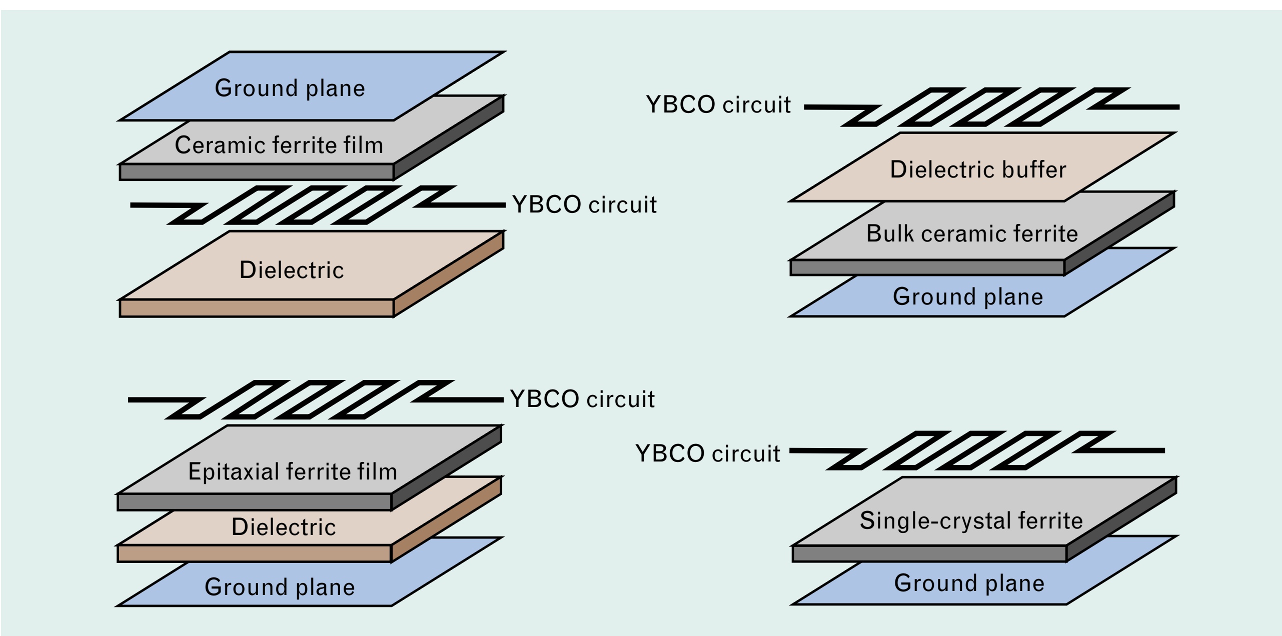

FIGURE 16. Four proposed arrangements for materials integration by layering ferrites and high-T_c superconductors. The purpose of these arrangements is to optimize the interaction between the ferrite and the superconductor.

ferred technology, notwithstanding the added cost and complications of a cryogenic enclosure. For filter-bank selector applications that would employ the ring-network circulator device, these issues also apply, and can include even larger bandwidths and switching speeds. For implementation of low-loss ferrite-superconductor phase shifters, circulator switches, and other devices that can utilize this low-loss principle, the adoption of cryogenically cooled array antennas is also an important step and should be treated as part of the system design where appropriate.

Acknowledgments

The authors are grateful to the Lincoln Laboratory Innovative Research Program Committee for its support in this exploratory project. The authors are also indebted to R.P. Konieczka, D.J. Baker, L.S. DiPalma, J.F. Fitzgerald, C.D. Hoyt, D.L. Hovey, R.J. Magliocco, and C.M. Vanaria for technical assistance throughout the course of this work. Dr. A.C. Anderson provided the YBCO films. We give a special acknowledgment to Dr. L.M. Johnson for his helpful assistance in the preparation of this article. This work was sponsored by the Department of the Air Force.

REFERENCES

1. H. Piel, H. Chaloupka, and G. Müller, "High Temperature Superconductors in High Frequency Fields—Fundamentals and Applications," *Advances in Superconductivity: Proc. 4th Int. Symp. on Superconducting, Vol. 4, Tokyo, 14–17 Oct. 1991*, pp. 925–930.
2. M.S. Pambianchi, D.H. Wu, L. Ganapathu, and S.M. Anlage, "DC Magnetic Field Dependence of the Surface Impedance in Superconducting Parallel Plate Transmission Line Resonators," *IEEE Trans. Appl. Supercond.,* vol. 3, no. 1, pp. 2774–2777 (1993).
3. E. Denlinger, R. Paglione, D. Kalokitis, E. Belohoubek, A. Piqué, X.D. Wu, T. Venkatesa, A. Fathy, V. Pendrick, S. Green, and S. Mathews, "Superconducting Nonreciprocal Devices for Microwave Systems," *IEEE Microw. Guid. Wave Lett.,* vol. 2, no. 2, pp. 449–451 (1992).
4. B. Lax and K.J. Button, *Microwave Ferrites and Ferrimagnetics* (McGraw-Hill, New York, 1962), pp. 150–157.
5. W.J. Ince and D.H. Temme, "Phasers and Time Delay Elements," *Advances in Microwaves, Vol. 4,* L. Young, ed. (Academic Press, New York, 1969), pp. 1–189.
6. G.F. Dionne, D.E. Oates, and D.H. Temme, "Low-Loss Microwave Ferrite Phase Shifters with Superconducting Circuits," *1994 IEEE MTT-S Int. Microw. Symp. Dig., Vol. 1, San Diego, 23–27 May 1994,* pp. 101–103.
7. F.J. Rosenbaum, "Integrated Ferrimagnetic Devices," *Advances in Microwaves, Vol. 8,* L. Young and H. Sobul, eds. (Academic Press, New York, 1974), pp. 203–294.
8. S.K. Koul and B. Bhat, *Microwave and Millimeter Wave Phase Shifters, Vol. 1* (Artech, Boston, 1991), pp. 338–347.
9. E.R.B. Hansson, S. Aditya, and M.A. Larsson, "Planar Meanderline Ferrite-Dielectric Phase Shifter," *IEEE Trans. Microw. Theory Tech.,* vol. 29, no. 3, pp. 209–215 (1981).
10. G.F. Dionne, D.E. Oates, and D.H. Temme, "Ferrite-Superconductor Microwave Phase Shifters," *IEEE Trans. Magn.*, vol. 30, no. 6, pp. 4518–4524 (1994).
11. G.F. Dionne, D.E. Oates, and D.H. Temme, "YBCO/Ferrite Low-Loss Microwave Phase Shifter," *IEEE Trans. Appl. Supercond.*, vol. 5, pp. 2083–2086 (1995).
12. G.F. Dionne, D.E. Oates, D.H. Temme, and J.A. Weiss, "Ferrite Superconductor Devices for Advanced Microwave Applications," *IEEE Trans. Microw. Theory Tech.,* vol. 44, no. 5, pp. 1361–1368 (1996).
13. A. Piqué, K.S. Harshavardhan, J. Moses, M. Mathur, E. Belohoubek, T. Venkatesan, E.J. Denlinger, D. Kalokitis, A. Fathy, V. Pendrick, M. Rajeswari, and W. Jiang, "Microwave Compatible $YBa_2Cu_3O_{7-x}$ Films on Ferrimagnetic Garnet Substrates," *Appl. Phys. Lett.,* vol. 67, no. 12, pp. 1778–1780 (1995).
14. B. Lax and K.J. Button, *Microwave Ferrites and Ferrimagnetics* (McGraw-Hill, New York, 1962), pp. 540–544.
15. B. Lax, "Frequency and Loss Characteristics of Microwave Ferrite Devices," *Proc. IRE*, vol. 44, pp. 1368–1386 (Oct. 1956).
16. G.T. Roome, "Thin Ferrites for Integrated Microwave Devices," Tech. Rept. AFAL-TR-69-149, Air Force Systems Command, Wright Patterson Air Force Base; also described in Ref. 7.
17. J.A. Weiss, "Circulator Synthesis," *IEEE Trans. Microw. Theory Tech.,* vol. 13, no. 1, pp. 38–44 (1965).
18. S.D. Ewing and J.A. Weiss, "Ring Circulator Theory, Design and Performance," *IEEE Trans. Microw. Theory Tech.,* vol. 15, no. 11, pp. 623–628 (1967).
19. J.A. Weiss and G.F. Dionne, "Performance Capabilities of the Ring Network Circulator for Integrated Circuits," *1995 MTT-S Int. Microw. Symp. Dig., Vol. 2, Orlando, FL, 15–19 May 1995,* pp. 725–728.
20. J.A. Weiss, G.F. Dionne and D.H. Temme, "The Ring Network Circulator for Integrated Circuits: Theory and Experiments," *IEEE Trans. Microw. Theory Tech.,* vol. 43, no. 12, pp. 2743–2748 (1995).
21. G.F. Dionne, "Properties of Ferrites at Low Temperatures," *J. Appl. Physics,* vol. 80, pp. 5064–5069 (1997).

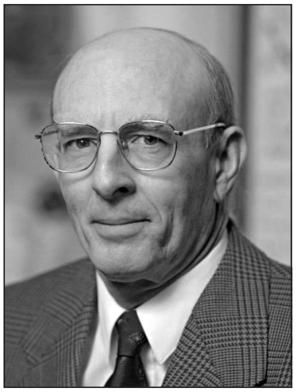

GERALD F. DIONNE
is a member of Expert Service Personnel, supporting the Analog Device Technology group. He received a B.Sc. degree (summa cum laude) in physics from the Université de Montréal (Loyola College), a B.Eng. degree in engineering physics from McGill University, an M.S. degree in physics from Carnegie-Mellon University, and a Ph.D. degree in physics from McGill University. He served as a member of the physics faculty at McGill University, worked on semiconductor device development with both IBM and the Sylvania Division of GTE, and researched electron emission and cesium vapor ionization for thermionic energy conversion at Pratt & Whitney Aircraft. Since 1966 he has carried out research at Lincoln Laboratory, where he has published extensively in fields that include magnetism theory and properties of ferrimagnetic materials for microwave, millimeter-wave, and magnetooptical applications, secondary electron emission, and millimeter-wave and submillimeter-wave radiometry. From his studies of the role of large polarons in high-T_c superconductivity, he recently developed an effective model for giant magnetoresistance effects. He has authored patents on microwave ferrite and superconductor devices. He is a Fellow of the IEEE and a member of the American Physical Society and the Society of Sigma Xi.

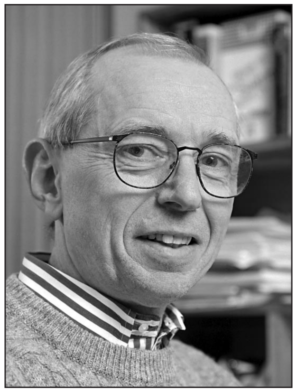

DANIEL E. OATES
is a staff member in the Analog Device Technology group. He received a B.A. degree from Yale University and a Ph.D. degree from MIT, both in physics. In 1971 he held an Alexander von Humboldt fellowship at the University of Bonn, Federal Republic of Germany, and from 1973 to 1978 he worked at Bell Telephone Laboratories. Since 1978 he has been a staff member at Lincoln Laboratory, where his research has included investigations of surface-acoustic-wave and bulk-acoustic-wave devices. Since 1988 his primary research interests have been in superconducting electronics utilizing the newly discovered high-transition-temperature materials, especially for applications in frequency control and microwave-frequency analog signal processing. Motivated by the potential applications of superconductors, he also has investigated the fundamental properties of superconductors at microwave frequencies and at high microwave power levels. These investigations have included both high-T_c and low-T_c materials. He is a member of the IEEE and the American Physical Society.

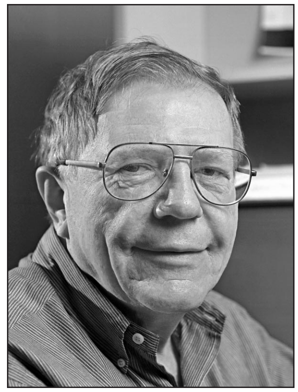

DONALD H. TEMME
is a former senior staff member in the Communications division, and is now a consultant to the Analog Device Technology group. His research specialty is in ferrite-superconductor control devices. He received a B.S. degree in electrical engineering from the University of Nebraska and an S.M. degree in electrical engineering from MIT. Before joining Lincoln Laboratory in 1957, he was in the U.S. Air Force. He is a Life Member of the IEEE and a member of Sigma Xi.

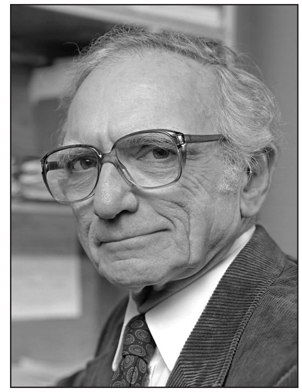

JERALD A. WEISS
is a consultant in the Analog Device Technology group. He received B.A., M.A., and Ph.D. degrees, all in physics, from The Ohio State University. In 1953 he joined the Bell Telephone Laboratories (now Lucent Technologies, Inc.) as a member of the technical staff, and he worked in the development of microwave component principles and devices with applications of magnetic materials. In 1962 he joined the physics faculty at Worcester Polytechnic Institute, where his work included teaching and research in microwave spectroscopy and the measurement and applications of gyrotropic and dielectric materials. He was appointed Professor Emeritus in 1988. In 1962 he also was appointed consultant to Lincoln Laboratory for work on materials and components relating to radar development, and he continues to serve in that role. He is the author of numerous publications and patents in areas including nonreciprocal microwave and millimeter-wave devices, transmission-line theory, and magnetic measurements. He is a member of Phi Beta Kappa, Sigma Xi, and the American Physical Society, and he is a Life Fellow of the IEEE.